2023

Development of holographic optical elements for use in wound monitoring

Pamela Stoeva
Technological University Dublin, pamela.stoeva@tudublin.ie

Tatsiana Mikulchyk
Technological University Dublin, tatsiana.mikulchyk@tudublin.ie

Brian Rogers
Technological University Dublin, brian.rogers@tudublin.ie

See next page for additional authors

Funder: European Space Agency, through PEA 4000129503 collaborative project: Wound Healing In Space: Key challenges towards Intelligent and Enabling Sensing platforms.

Development of holographic optical elements for use in wound monitoring

P. Stoeva [a,b], T. Mikulchyk [a,b], B. Rogers [a,b], M. Oubaha [c], S. Martin [a,b], D. Cody [a,b], M.A. Ferrara [d], G. Coppola [d] and I. Naydenova [a,b*].

[a] Centre for Industrial and Engineering Optics, School of Physics, Clinical and Optometric Sciences, TU Dublin, Grangegorman, Ireland.

[b] The FOCAS Research Institute, TU Dublin, 13 Camden Row, Ireland, D08 CKP1.

[c] CREST, TU Dublin, 13 Camden Row, Ireland, D08 CKP1.

[d] ISASI-NA, 70, Via Pietro Castellino 111, 80131 Naples, Italy.

*Izabela.naydenova@tudublin.ie.

ABSTRACT

Wounds that fail to heal impact the quality of life of 2.5 % of the total population. The costs of chronic wound care will reach $15–22 billion by 2024. These alarming statistics reveal the financial strain for both the medical industry and society. A solution can be found in compact and accessible sensors that offer real-time analysis of the wound site, facilitating continuous monitoring and immediate treatment, if required. Benefits of these sensors include reduction of cost and can extend the reach of healthcare to remote areas. The progression of a wound site can be closely monitored with holographic optical elements (HOEs) by real-time quantification of wound healing biomarkers, such as oxygen, temperature, pH and lactate. Fabrication of such wound monitoring sensors requires biocompatible, water-resistant photosensitive materials suitable for specific functionalisation with respect to wound analytes.

Here, the design and fabrication of a HOE for delivering an excitation light beam to the sample chamber of a photoluminescence-based wound monitoring system is reported. We present a photopolymerisable hybrid sol gel (PHSG) material, capable of recording a 60 % diffraction efficiency holographic waveguide. A 1692 ± 5 lines/mm slanted transmission HOE has been theoretically designed and fabricated in PHSG films to in-couple a 633 nm beam into the oxygen sensing site. An identical grating has been used to out-couple the 633 nm beam out of the system. Stability of the PHSG grating post 476.5 nm recording was achieved by two techniques, 532 nm uniform illumination and UV-curing. The unform exposure to laser light was proved to be the more successful method since UV exposure was demonstrated to result in layer damage due to accumulated stress. The potential of waveguides as light filtering optical elements is also explored.

Keywords: Holographic waveguide; in- and out-coupling; oxygen sensing; wound monitoring; photopolymerisable glass; photopolymerisable hybrid sol gel

1. INTRODUCTION

Chronic wounds, which are persistent non-healing cuts to the skin, can significantly impact a person's quality of life, lead to disability, and contribute to healthcare costs[1], making their prevention and effective treatment of utmost importance. By offering precise evaluation of the wound site, sensors can provide a platform that will alleviate the symptoms and prevent the onset of chronic inflammation, enabling prompt diagnosis and effective treatment. Wearable, reusable, biocompatible and fast-responsive sensors with real-time monitoring can provide relief to the healthcare system and the victims of wounds. Fundamental biochemical mechanisms regulating wound healing are typically related to elementary parameters, such as, oxygen, pH, temperature, and lactate concentration[2]. Detailed quantification of these biomarkers can reveal the extent of recovery at a wound site; typical values for indication of infection for each biomarker are summarised in figure 1. Holographic optical elements (HOEs) are suitable candidates for wound healing monitoring, both as an independent sensing system and, as an optical element to guide the probe beam in/ out of a wound sensing system. HOEs feature diverse sensing capabilities, physical properties (i.e., lightweight, flexible, and compact) and suitability for mass manufacturing[3].

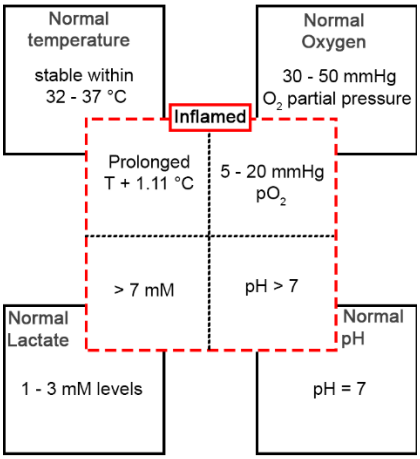

Figure 1. Diagram showing indicators of infection for temperature, oxygen, lactate, and pH.

The key wound healing indicator of interest to the work presented here is Oxygen (O_2). O_2 is a critical chemical biomarker that contributes to the wound healing process by participating in essential biochemical energy supply. Like most processes in organisms, biochemical energy supply is also vital for wound healing. O_2 sustains the production of biological energy through various methods (i.e., aerobic glycolysis, citric acid cycle and oxidation of fatty acids), maintaining an adequate environment for normal cellular functionality[4]. High energy demand in healing tissue is demonstrated in fundamental reparative processes such as, bacterial defence, cell proliferation and collagen synthesis[4]. Hence, the ability to monitor partial pressure of dissolved Oxygen (pO_2) at a wounded site in real-time can offer key information about the healing tissue. Healthy tissue demonstrates pO_2 in the range of 30 - 50 mmHg and inflammation at the site is indicated by the lower range, 5 – 20 mmHg[4].

Oxygen sensing sites based on excitation and subsequent photoluminescence are of particular interest to the work described here. By utilizing oxygen quenching luminescent dyes, traditional luminescence-based O_2 sensors can reliably measure available oxygen concentration through collisional quenching[5], which impacts the intensity of emitted luminescence, thereby making the technique an effective sensor. Holographic waveguides can assist luminescence-based oxygen systems by providing and/or collecting a light signal from the photoluminescent sensing region. HOEs can capture multiple optical functions in a single component. The holographic technique allows for complex beam interference patterns to be stored in a photosensitive medium. When a propagating beam interacts with the HOE, the light will be guided based on the stored diffraction pattern. In this work, we design a HOE for delivering an excitation light beam to the sample chamber of an oxygen sensing site and optimise its fabrication in a photosensitive sol-gel material. The post-recording treatment has been further optimised to stabilise the HOE properties over time. The ability of recording a double holographic coupler – one to guide the light into the chamber and a second one to redirect the coupled light into a photodetector has been demonstrated.

2. DESIGN OF THE HOLOGRAPHIC COUPLERS

For this application, a volume phase hologram with a specific periodicity and slant angle is designed to redirect the excitation wavelength of the O_2 sensing site into the system at the critical angle (θ_c) or larger, suitable for total internal reflection (TIR) as visualised in step (1) in figure 2. The TIR beam should propagate through the system, striking and exciting the sensing region as seen in step (2). The excited site will emit light in every direction, like a point light source, where 23 % of the light will naturally experience TIR in agreement with the critical angle theory in opposite directions, step (3) figure 2. In the final step (4), a similar HOE structure will be modelled to guide the naturally coupled luminescence out of the system for O_2 measurements relevant to the healing wound environment. In this study, two HOEs are required; the first HOE directing the light into the system is the in-coupler and the second HOE extracting the light out of the system is the out-coupler.

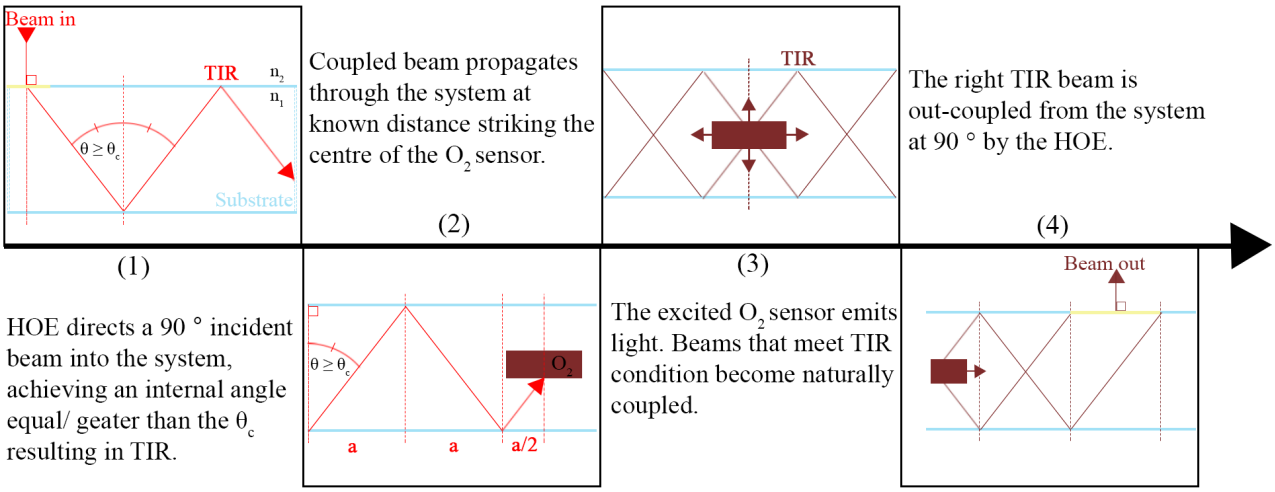

Figure 2. Flowchart showing the four key steps in providing and extracting a signal from a luminescence based O2 sensor with HOE waveguides.

To simplify the optical path and minimise beam losses, a HOE operating in transmission mode is modelled as the waveguiding component for the oxygen sensing system. In order to transmit the beam into the system at an angle suitable for TIR, a slanted grating was considered. This paper utilises a recording technique recently published by Chakraborty et al.[6] which benefits from recording of the holographic waveguide at a shorter wavelength for operation at a longer wavelength. The same approach was implemented here, to the best of our knowledge for the first time, to record two waveguides (in-coupler and out-coupler) in a sol-gel material. The two couplers are to be integrated into a photoluminescence-based oxygen sensing system for wound healing monitoring. Briefly, the dye excitation wavelength and the critical angle for TIR were used in the calculation of the characteristic spatial frequency (SF) of the operating holographic waveguide. In the recording setup, a shorter wavelength was used to make it possible for the beams to enter the photosensitive material. The Bragg angle of the recording wavelength was calculated for the known SF and used in the recording optical setup.

Modelling of the waveguide revisits the concept of total internal reflection which relates the refractive index of the two interacting mediums (external material, n_2, and internal material, n_1) to determine the minimum critical angle (θ_c) for coupled propagation within the layer of interest:

$$\theta_c = \sin^{-1}\frac{n_2}{n_1} \tag{1}$$

The period of the slanted grating with the required θ_c is determined by:

$$\Lambda = \frac{\lambda_i}{2\, n_1\, sin\,(\frac{\theta_1 - \theta_c}{2})} \tag{2}$$

where λ_i is the wavelength of illumination and θ_1 is the desired angle of incidence for the reconstruction of θ_c. Since the reconstruction beam is to be incident on the grating at 90 ° in air, a shorter wavelength is required for the recording process to ensure that the recording beam enters the photosensitive layer. Once the required period of the structure is determined, it is possible to determine the angle between the two recording beams ($2\theta_r$) of a chosen shorter wavelength (λ_r) using equation (3)

$$\theta_r = 2\,\sin^{-1}\frac{\Lambda\, 2\, n_1}{\lambda_r} \tag{3}$$

Finally, the differences in the incident angles for the recording (λ_r) and reconstruction (λ_i) wavelengths are calculated for air using Snell's law and then integrated into the optical set up visualised in the schematic presented in figure 3.

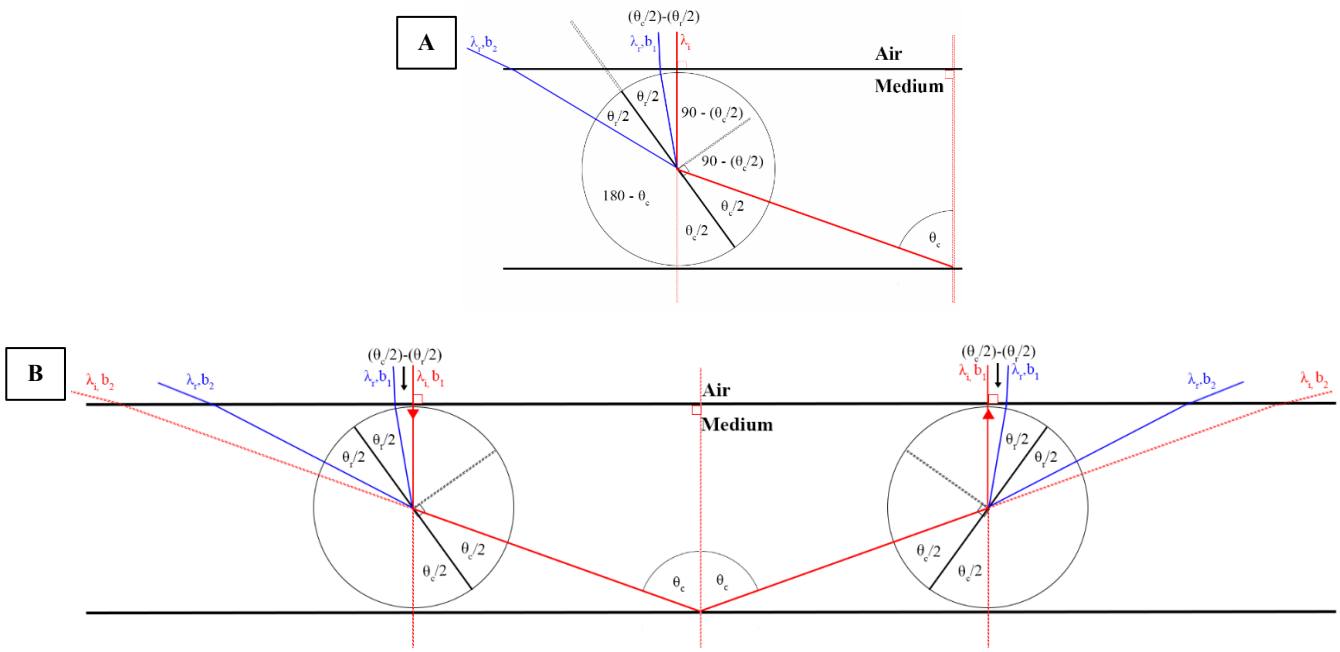

Figure 3. Schematic of model used for the determination of the recording angles in the optical set up:
(A) Diagram demonstrates the model for a single waveguide system; in-coupler.
(B) Diagram demonstrates the model for two waveguide system: in- and out-coupler.

3. MATERIALS AND METHODS

3.1 PHSG solution preparation

The four-step solgel development process recently detailed[7] was utilised with modifications to synthesise a photopolymerisable hybrid sol gel. Two hybrid precursors, MAPTMS and a ZPO complex (ZCO), were employed for the four-step synthesis. The first step involved, (a) the complexation of ZPO to ZCO in the presence of MAA following 45-minute mixing time. In parallel, (b) the hybrid silicate matrix was developed after 45-minute mixing of MAPTMS with HNO_3. The second step involved mixing both solutions (MAPTMS/ HNO_3 and ZPO/MAA) together for 5 minutes in a glass container. Dropwise addition of deionised water followed in step three, and the sol base was then stirred for 24 hours at ambient conditions. The final step, step four, included the addition of modifiers such as APTES, Omnirad 784 and isopropanol into 10 g of the sol base developed at step 1-3. Finally, after another 10 hours of stirring the photosensitive hybrid sol-gel matrix was complete. The chemicals used were purchased from Merck (HNO_3, ZPO, MAA and APTES), Safic Alkane (MAPTMS) and IGM Resins (Omnirad 784) and their volumes are presented in table 1.

Table 1: Chemical component amounts and concentrations used in the development of PHSG the hybrid sol gel.

Components for sol base	**Amount (g)**
MAPTMS, 3-trimethoxysilylpropyl methacrylate	15.000
HNO_3, Nitric acid	1.600
ZPO, Zirconium (IV) propoxide	0.727
MAA, Methacrylic acid	0.135
H_2O, Deionised water	1.088

Modifiers	Concentration (% w/w)
APTES, (3-aminopropyl) triethoxysilane	4.5
Omnirad 784, Bis(eta.5-2,4-cylcopentadien-1-yl)-bis(2,6-difluoro-3-(1H-pyrrol-1-yl)-phenyl) titanium	0.5
Izopropanol	31

3.2 Photosensitive layer preparation

Fresh (0-day) sol-gel solution was drop-casted onto a levelled half glass slide (37.5 x 25 mm^2, 1 mm thick) in a dark room. The layers were then dried in the oven (Binder, model ED56) for a period of 45 minutes, yielding dry layers with thickness of 150 μm ± 50 μm.

3.3 Recording setup

The recording geometry was arranged for the recording of holographic in- and out- couplers with a spatial frequency (SF) of 1692 ± 5 lines/mm. Two 476.5 nm laser beams (Argon ion laser model 95) were incident on the photosensitive layer at equal - 27.5˚ and + 27.5˚ to the normal of the layer surface for recording an unslanted grating. For the recording of the slanted gratings, the layer was rotated with respect to the two recording beams in such a way that one of them was incident at 8˚ to the normal, and the second beam was incident at 63˚. The recording intensity was varied between 2 – 12 mW/cm^2 and exposure times of 20 – 80 s were used for the determination of the optimal recording conditions.

3.4 Probing setup

Bragg selectivity curves were generated post recording with a computer supported setup controlled by an in-house developed LabVIEW programme. The setup consisted of a rotational stage linked to a motion controller (Newport ESP300) and an optical power meter (Newport model 843-R) detecting the intensity of the 633 nm transmitted beam as the grating rotates through the Bragg angle. The diffraction efficiency (DE) of the recorded gratings was calculated as the ratio of the intensity of light diffracted by the grating to the intensity of light incident on the grating. Coupling was observed after probing at normal incidence to the grating using a 633 nm, He-Ne laser beam (1.6 mW/cm^2).

White light was coupled into the axis of the PHSG waveguide sample by aligning a collimated Halogen white lamp (AvaLight-HAL-S) beam perpendicular to the side of the sample. The transmitted red beam was characterised with the AvaSpec 2048 USB powered spectrometer connected to the Ava soft 7.5 software.

4. RESULTS AND DISCUSSION

4.1 Optimization of the recording conditions for the PHSG- holographic waveguide

First, the influence of recording exposure energy on the diffraction efficiency of slanted volume transmission gratings fabricated in the PHSG was investigated. The diffraction efficiency values plotted in figure 4 are for holographic waveguides recorded using the same exposure time but different recording intensities. The selection of intensities (2.5, 5, 10 and 12.5 mW/cm^2) utilised for the recording process led to the recording of couplers with diffraction efficiency ranging between 40 and 51 % (figure 4). This implies that within the studied intensity range there is no evident exposure energy dependence of the recording process in the sol-gel samples under study.

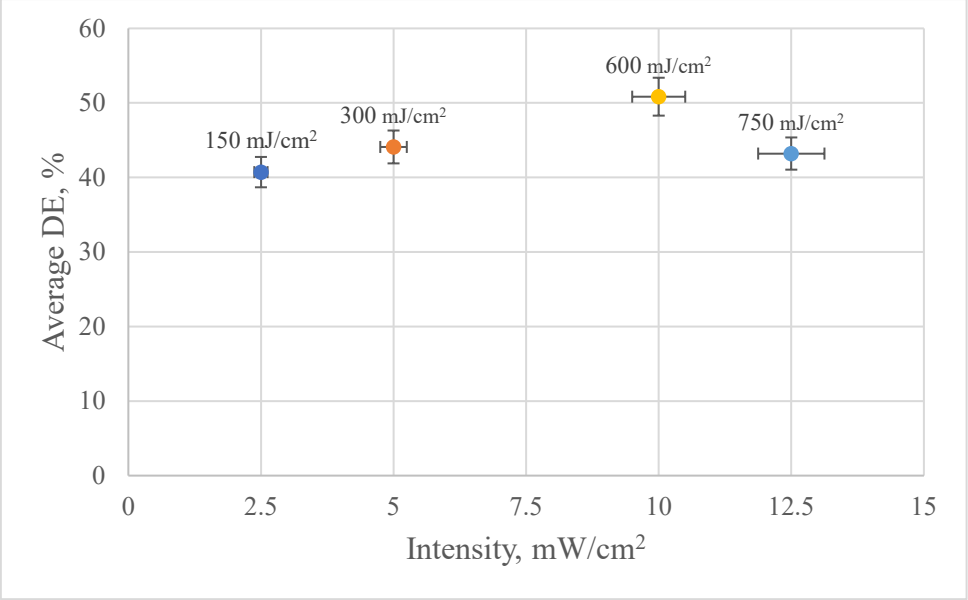

Figure 4. DE versus total recording intensity of the 476.5 nm beams, at a fixed exposure time of 60 s and the corresponding energy values and the error y-axis error bars represent the standard deviation on the average of 3 measurements.

Optimisation of the recording exposure times was then investigated. An intensity of 3 mW/cm^2 was used with exposure times varying from 20 – 80 s. Diffraction efficiency fluctuations in the range of 25 – 45 % are evident in figure 5 for the selected energy conditions with no evident trend. Overmodulation for exposure times greater than 60 s was noted in the Bragg curves. Since an average DE of the gratings recorded in the sol-gel layer was achieved to be in the order of 40 %, at the lower range of supplied energy, these recording conditions were selected for further studies. Finally, figure 6 shows a schematic and demonstrative photograph of the operation of the slanted transmission gratings as holographic in-couplers.

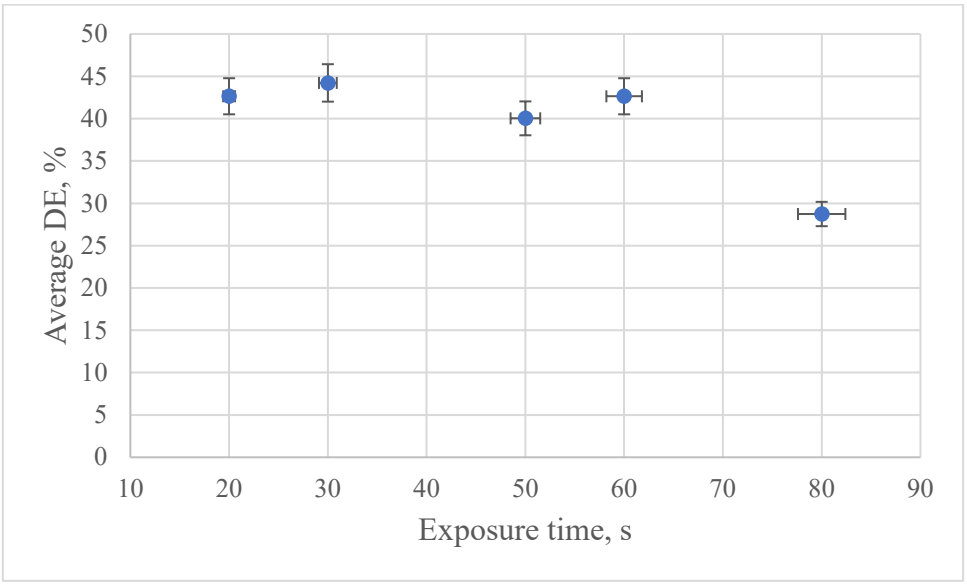

Figure 5. Plot of the average diffraction efficiency recorded at the relevant exposure times at for a fixed intensity of 3 mW/cm^2 for 0.50 ml layers (150 ± 50 µm).

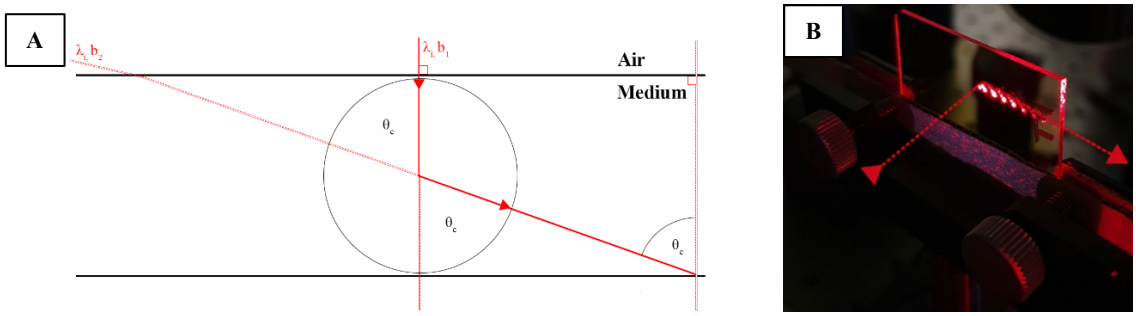

Figure 6. (A) Schematic of in-coupler operation and, (B) Image of recorded and operating PHSG holographic waveguide.

4.2 Effect of PHSG grating aging on its properties

The aging of the PHSG and its effects on the recording properties of the layers have been explored in a recent publication [8]. The investigation in this section includes an in-depth analysis of modifications that occur to the photonic structure over time post recording. The experimental set up for monitoring the aging process of the gratings employs Bragg selectivity measurements. Analysis of the Bragg curves of the slanted PHSG gratings post recording revealed non-reversible structural changes to the gratings as they aged. Only 0.25 hours (15 minutes) post recording, changes in the optical characteristics of the gratings occur, as illustrated in the Bragg curves in figure 7(A). The Bragg angle of the grating exhibits a 0.35 ° shift, a 15 % diffraction efficiency decrease, and curve broadening.

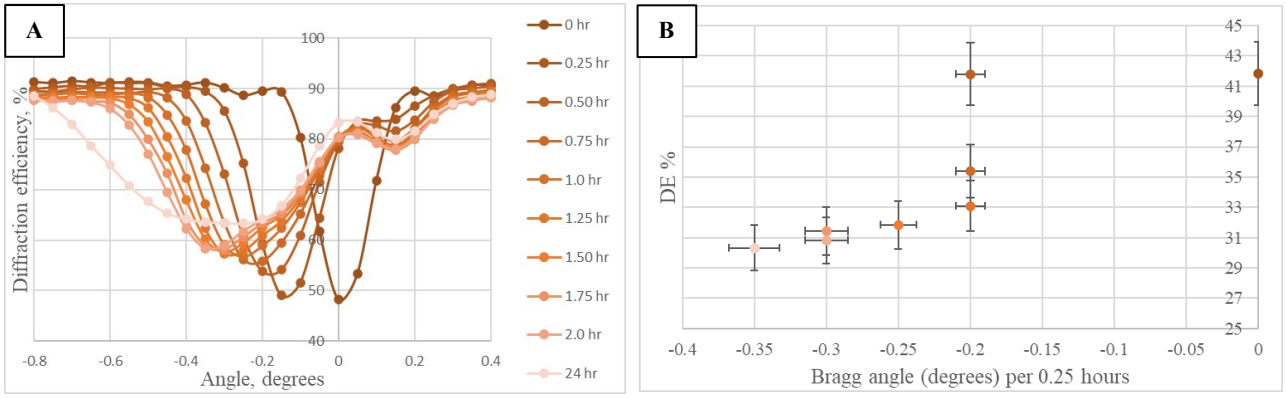

Figure 7. (A) Bragg selectivity curves of a grating recorded for 20 s with recording intensity 3 mW/cm^2 and probed post recording every 0.25 hr for 2 hours, and after 24 hours.

(B) Diffraction efficiency vs. peak Bragg angle as obtained every 0.25 hrs for the same grating.

These shifts proceed for the full 24-hour period, showing that there is a change in the properties of the recorded structure. Data obtained from the Bragg curves in figure 7(B), demonstrates consistent change of the DE and Bragg angle every 0.25 hrs for the recording conditions of 20 s at 3 mW/cm^2.

4.3 Dark process stabilisation

The combination of physicochemical processes that occur post recording of the PHSG-based gratings have been recognised as dark processes that proceed without light. These dark processes are evident in the Bragg selectivity curves (figure 7) discussed in 3.2. Broadening of the curves, angular shift of the grating fringes from Bragg angle and DE changes suggest dimensional and/or physiochemical processes that proceed even after holographic exposure. Diffraction efficiency decreases is particularly problematic for such PHSG-based holographic couplers and their application in the intended light guiding applications. Thus, stabilisation of the grating characteristics to stop its aging is necessary.

Generally, Class I photopolymerisable systems [9] (hybrid organic-inorganic materials) exhibit enhancement of the refractive index modulation during this dark stage due to proceeding diffusion of monomers and high refractive index species [7]. The absence of covalent bonds between the silicate matrix and both monomers and high refractive index species in the Class I

compositions accommodate for this diffusion. The studied material in this work is based on a novel PHSG[7] that is categorised as a Class II photopolymerisable glass, where strong organic and inorganic bonds are noted and as a result limited diffusion is expected. Polycondensation processes are thought to be the dominant factor in the formation of gratings in PHSG during the dark process. The polycondensation processes influence refractive index modulation and hence DE changes for hours post recording[8].

Post–recording UV-curing was used to study elimination of the dark process effects influencing refractive index modulation and diffraction efficiency variations. UV-curing increases the density of the layer due to enhanced polymerisation which in turn increase material robustness[9]. Slanted transmission gratings were recorded with 3 mW/cm^2 exposure for 20 s at 476.5 nm. The recorded PHSG layers were immediately bleached with a Dymax UV-curing system (ECE Series) at 797, 5926 and 11852 mJ/cm^2 (Table 2) and the diffraction efficiency was measured as the grating aged (0 – 24 hr).

Table 2. UV- intensity and exposure time used to match three different energy conditions.

Intensity, mW/cm^2	Time (s)	Energy (mJ/ cm^2)
27	30	797
60	13	
27	223	5926
60	99	
27	446	11852
60	198	

Figure 8 demonstrates complete stabilisation of the DE maximum value after UV exposure, identical graphs were observed for all conditions. Angular drift of the Bragg angle is still evident in the range of a 0.25 ± 0.005 ° shift which is reduced compared to figure 7(A). The angular drift of the Bragg angle suggests that the material continues to experience dimensional change with time. This causes accumulation of stress between the material and substrate due to shrinkage of the coating. In addition to the stress, the enhanced robustness led to the development of surface fractures over time following high UV exposure observed in figure 9. Lower intensity of 5 mW/cm^2 with a shorter exposure time (5 minutes) of the UV light to the layer was also investigated via a UV Exposure Unit LV 202E. Layer fractures were again observed, and the energy (1500 mJ/cm^2) was not sufficient for grating stabilisation.

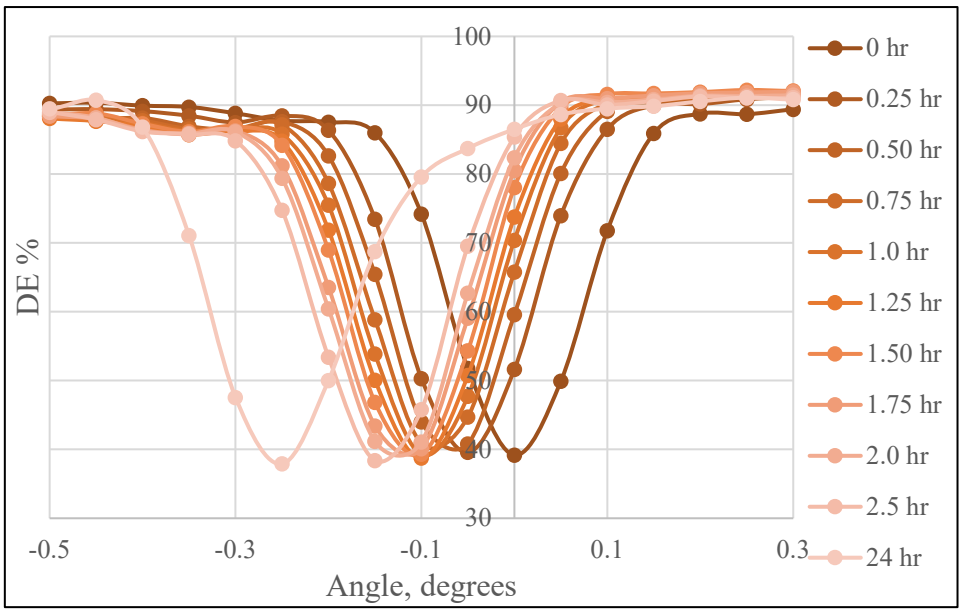

Figure 8. Bragg selectivity curves of sample cured at 5926.14 mJ/cm^2 for a period of 0 – 24 hr.

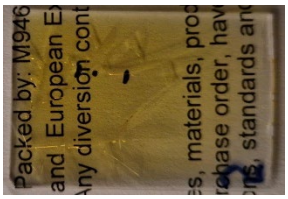

Figure 9. Shattered sol gel layer following post-recording UV-curing.

Further characterisation of the UV-cured and fractured grating was not possible due to high scattering, measuring a DE in the range of 0 – 5 %. While UV-curing of the layers can improve polymerisation and result in stabilised refractive index modulation, the associated changes in mechanical properties can be too significant. As a result, the benefits of stabilising diffraction efficiency through UV post-recording exposure are negated by the layer's mechanical instability and the development of fractures. A softer substrate that will accommodate for layer shrinkage was considered. A 500 µm polycarbonate (Bayer Makrofol DE1-1cc) films were successfully coated with 0.50 ml of the PHSG and subjected to the same UV-curing conditions. The flexible coated substrate further confirmed that the PHSG shrinks during the dark process which lead to curling in the direction of the UV-curing bulb. The curling made it impossible to assess the grating properties further.

Another investigation was designed with the aim to stabilise the optical structure immediately after recording. The study involved post-recording bleaching of the recording region with a 532 nm uniform beam. The gratings were subjected to uniform exposure of the beams for 300 s immediately after recording. The diffraction efficiency and angular position of Bragg was measured after that. Bleaching by illumination with a single 532 nm beam demonstrates promising stabilisation of the grating as seen in figure 10. There is an angular drift of 0.18 ± 0.005 ° from the Bragg angle and a DE decrease of 2 ± 0.0005 % following 1 week of aging. The aging of the DE has been reduced for gratings with recording conditions of 3 mW/cm^2 and 20 s at 476.5 nm and bleached via 532 nm.

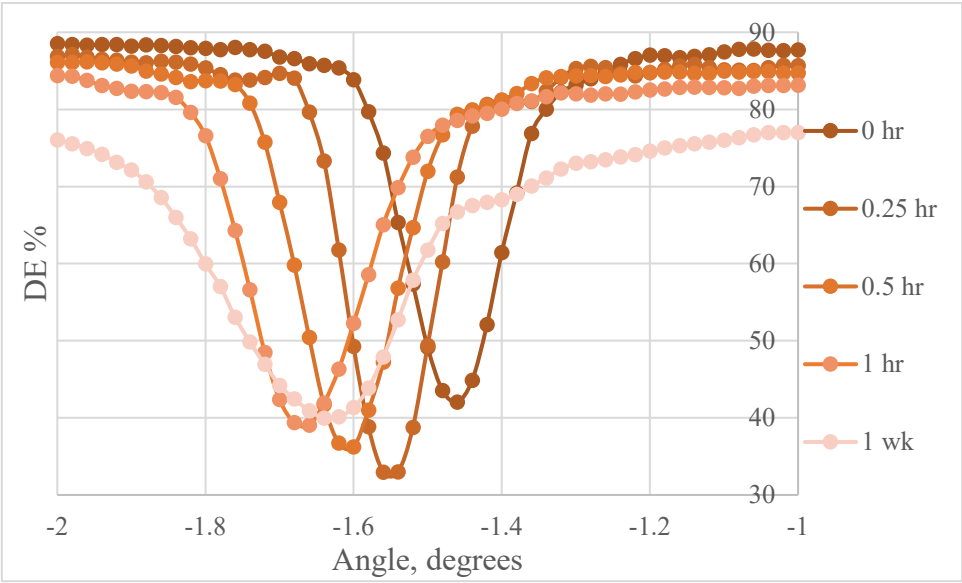

Figure 10. Bragg selectivity curves for an aging sample, following bleaching at 300 s, 3 mW/cm^2 with a 532 nm beam.

4.4 Functioning device model

The first purpose of the holographic waveguide is to couple light into a Polydimethylsiloxane (PDMS) microfluidic chamber system designed for oxygen detection based on photoluminescence. The sample chamber contains a dye that is sensitive to a 633 nm wavelength. The operation of the complete device is visualised in figure 11, where the 633 nm beam enters the device following interactions with the PHSG waveguide and propagates along the medium in the first part.

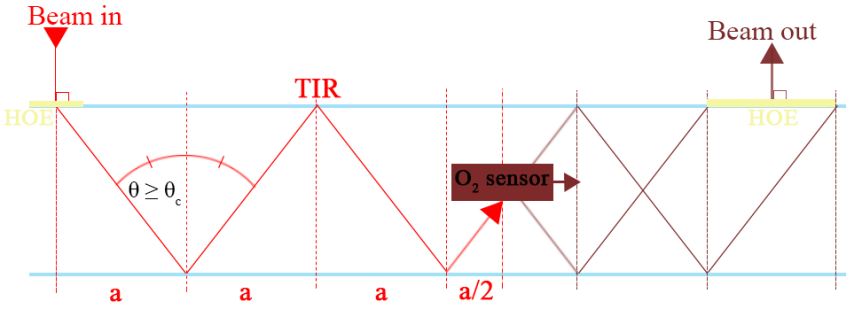

Figure 11. Schematic of beam path in the oxygen sensing system.

The light will bounce 'a' number of times and strike the centre of the sensing region of the system. The number of bounces within the medium are directly related to the angle at which the light will be directed into layer, the thickness of the layer and position of the sensor. Where each bounce can be associated with an intensity loss of the propagating exciting beam. Corresponding number of bounces N of the beam before reaching the chamber can be estimated from equation 4:

$$N = \frac{D}{h * \tan\theta} \tag{4}$$

D is the distance from the centre of the HOE to the centre of the sensor chamber, h is the height of the system and θ is an angle that meets TIR ($\theta \geq \theta_c$). The relationship shows how the number of bounces can be minimised by increasing the angle at which the incident beam is diffracted by the HOE. This can be utilised to help reduce intensity losses of the propagating signal.

To demonstrate the out-coupling ability of the PHSG waveguide in our lab, the recorded grating layer was oriented to record another identical 1692 ± 5 lines/mm waveguide on the same axis, with mirrored slants (figure 3(B)). This device coupled a collimated 633nm beam, incident along the sample normal, into the layer, visualised in figure 12(A). As seen in figure 12(B), after a number of bounces the beam reaches the second coupler at 42 ± 0.5 ° and is coupled out from the system.

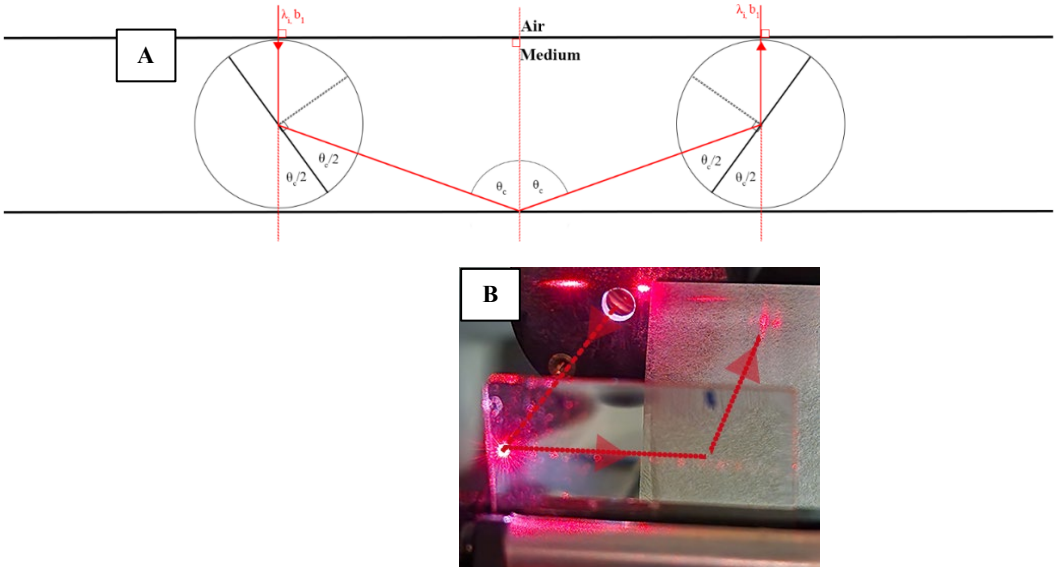

Figure 12. (A) Schematic of the two-waveguide system.
(B) Coupling the beam in and, out-coupling after normal incidence onto the first coupler and 42 ° incidence onto the second coupler. Exiting beam is observed on the white screen.

4.5 Waveguide as a filter

Since the characteristic spatial frequency of a HOE structure is dependent on the wavelength and Bragg angle, reconstruction will only be seen when these two conditions are met. The holographic waveguide developed in this study has a SF that when illuminated with a 633 nm beam at 90 °, it reconstructs at 42 ° and vice versa. Theoretically, if white light was incident onto the grating at either 90 or 42 °, a 633 nm beam should be filtered out and reconstructed at either 42 or 90 °, respectively. This waveguide behaviour has also been similarly explored by Fernandez et al.[10]. The waveguides functionality as a filter, in this work, was studied by sending a collimated light beam from a Halogen lamp along the axis of the sample. When the beam was coupled within the substrate, at the region containing the recorded HOE coupler a red beam was seen coming out at 90 ° (figure 13(A)), confirming the potential of waveguides as light filtering optical elements (figure 13(B)).

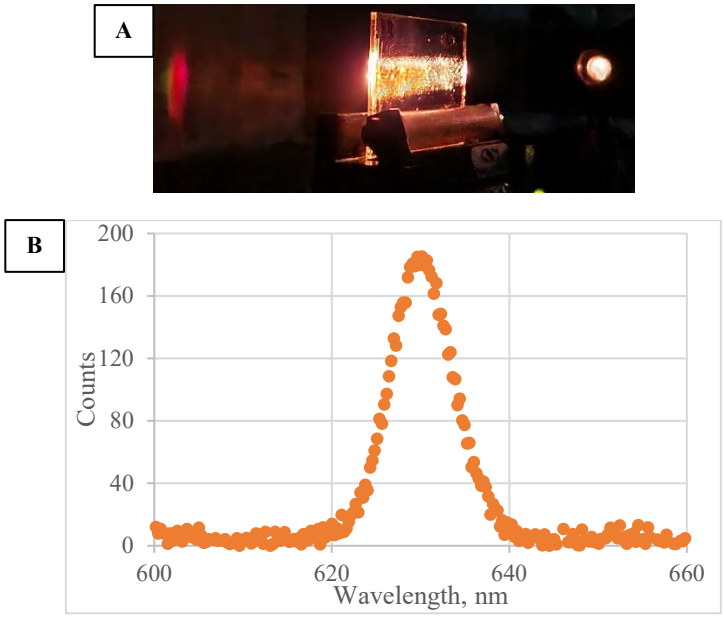

Figure 13. (A) Image of white beam coupled within PHSG sample, and a 663 nm beam filter out by the grating. (B) Spectrum of the filtered beam confirming the 633 nm peak wavelength.

5. CONCLUSION

This paper presented the successful development of a holographic waveguide in a novel photopolymerisable hybrid sol-gel material. A technique utilising a lower wavelength of recording for couplers to operate at a longer wavelength was demonstrated[6]. Recording conditions of 3 mW/cm^2 at 20 s using a 476.5 nm recording beams revealed 60 % diffraction efficiency when the waveguide is probed with a 633 nm beam at normal incidence to the layer. Waveguide stability was achieved by single 532 nm beam illumination of the grating region at an intensity of 3 mW/cm^2 and 300 s exposure time. Diffraction efficiency stability for these samples has so far been observed for a minimum of 7 days. Wavelength filtering properties of the coupler were also demonstrated. Both in-coupling and out-coupling capabilities of the holographic optical element have been demonstrated. In conclusion, the PHSG holographic waveguide exhibits promising features that can prove useful in the field of optical sensing.

ACKNOWLEDGEMENTS

The work on this project has been funded by the European Space Agency, through PEA 4000129503 collaborative project: Wound Healing In Space: Key challenges towards Intelligent and Enabling Sensing platforms.

REFERENCES

[1] C. K. Sen, “Human wounds and its burden: An updated compendium of estimates,” *Advances in Wound Care*, vol. 8, no. 2, pp. 39–48, 2019.

[2] M. S. Brown, B. Ashley, and A. Koh, “Wearable Technology for chronic wound monitoring: Current dressings, advancements, and future prospects,” *Frontiers in Bioengineering and Biotechnology*, vol. 6, 2018.

[3] A. K. Yetisen, I. Naydenova, F. da Cruz Vasconcellos, J. Blyth, and C. R. Lowe, “Holographic sensors: Three-dimensional analyte-sensitive nanostructures and their applications,” *Chemical Reviews*, vol. 114, no. 20, pp. 10654–10696, 2014.

[4] S. Schreml, R. M. Szeimies, L. Prantl, S. Karrer, M. Landthaler, and P. Babilas, “Oxygen in acute and chronic wound healing,” *British Journal of Dermatology*, vol. 163, no. 2, pp. 257–268, 2010.

[5] B. A. DeGraff and J. N. Demas, “Luminescence-based oxygen sensors,” *Reviews in Fluorescence 2005*, pp. 125–151.

[6] D. Chakraborty, R. Georgiev, S. Aspell, V. Toal, I. Naydenova, D. Cody, and S. Martin, “Modelling and design of holographic optical elements for beam-coupling applications for a range of incident beam angles,” *Photonics*, vol. 9, no. 12, p. 936, 2022.

[7] T. Mikulchyk, M. Oubaha, A. Kaworek, B. Duffy, M. Lunzer, A. Ovsianikov, S. E-Gul, I. Naydenova, and D. Cody, “Synthesis of fast curing, water-resistant and photopolymerizable glass for recording of holographic structures by one- and two-photon lithography,” *Advanced Optical Materials*, vol. 10, no. 6, p. 2102089, 2022.

[8] T. Mikulchyk, P. Stoeva, A. Kaworek, M. Oubaha, B. Rogers, S. Martin, D. Cody, and I. Naydenova, “Characterisation of holographic recording in environmentally stable Photopolymerisable Glass,” *Applied Sciences*, vol. 12, no. 12, p. 5969, 2022.

[9] Ó. Martínez-Matos, M. L. Calvo, J. A. Rodrigo, P. Cheben, and F. del Monte, “Diffusion study in tailored gratings recorded in photopolymer glass with high refractive index species,” *Applied Physics Letters*, vol. 91, no. 14, p. 141115, 2007.

[10] R. Fernández, S. Bleda, S. Gallego, C. Neipp, A. Márquez, Y. Tomita, I. Pascual, and A. Beléndez, “Holographic waveguides in Photopolymers,” Optics Express, vol. 27, no. 2, p. 827, 2019.